

See discussions, stats, and author profiles for this publication at: <https://www.researchgate.net/publication/52006788>

# Electric Field Effects on the Adsorption of CO on a Graphene Nanodot and the Healing Mechanism of a Vacancy in a Graphene Nanodot

ARTICLE *in* THE JOURNAL OF PHYSICAL CHEMISTRY C · FEBRUARY 2012

Impact Factor: 4.77 · DOI: 10.1021/jp210719r

---

CITATIONS

17

---

READS

84

2 AUTHORS, INCLUDING:



Hongguang Liu

Jinan University (Guangzhou, China)

16 PUBLICATIONS 200 CITATIONS

SEE PROFILE

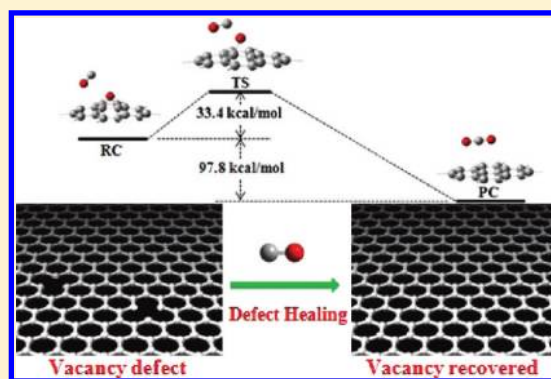
# Electric Field Effects on the Adsorption of CO on a Graphene Nanodot and the Healing Mechanism of a Vacancy in a Graphene Nanodot

Hongguang Liu<sup>†</sup> and Jin Yong Lee<sup>\*,†,‡</sup>

<sup>†</sup>Department of Chemistry, Sungkyunkwan University, Suwon 440-746, Korea

<sup>‡</sup>Supercomputing Center, Korea Institute of Science and Technology Information, Yuseong, Daejeon 305-806, Korea

**ABSTRACT:** It is well known that the external electric field can effectively modify the electronic structures and transport properties of low-dimensional systems. However, to our knowledge, the corresponding atomic structure and adsorption property changes of a graphene carbon network under different applied electric fields have not been investigated. Herein, using first-principles DFT calculations, we have systematically explored the CO adsorption on the pristine graphene nanodot and the defective one by taking the external electric field into account. It is found that the electric field can increase the CO adsorption energy and there is a barrier for CO–vacancy recombination that is mostly believed to remerge instantaneously when they come close to each other. Also, we proposed a mechanism for the subsequent healing of a monovacancy on a graphene nanodot by interaction with CO molecules, leading to the restoration of a pristine hexagonal carbon network.



## INTRODUCTION

Carbon-based materials, such as graphene and carbon nanotubes (CNTs), are the current focus of substantial research activity. CNTs, as one of the most promising candidates to replace silicon, have attracted intensive scientific interest due to their unique electrical, optical, and mechanical properties.<sup>1</sup> However, CNTs also have unsolved drawbacks, such as random orientation and spatial distribution, which largely suppress their real applications in life since most electronic devices require that they be connected.<sup>2</sup> Another famous star of carbon-based materials, graphene, a single atomic layer of graphite, is also regarded as an extremely promising candidate for electronic devices, due to its high carrier mobilities at room temperature ( $3000\text{--}27000\text{ cm}^2\text{ V}^{-1}\text{ s}^{-1}$ )<sup>3</sup> and large theoretical surface area ( $2600\text{ m}^2\text{ g}^{-1}$ ).<sup>4</sup> Because both graphene and CNTs benefit from their exceptional high carrier mobilities and large surface area, such characteristics open an avenue for inventing new gas sensors with higher sensitivity and faster response time.

Flourishing research activity has been driven to gain more sensitive, more accurate, and more reversible CNTs or graphene-based sensors,<sup>5</sup> while still not enough concerns have been paid to structural defects, which are commonly encountered during the current synthesis and characterization of carbon-based materials.<sup>6</sup> The presence of these defects can degrade the performance and reliability of such devices, because two important errors can be induced: the shift of the energy gap and under- or overbinding between the defect and the adsorbate.<sup>7</sup> The large-scale production of graphene sheets and CNTs with minimal defects or oxidation sites has been a barrier for commercial product development. Therefore, how to heal those defects and restore

the original properties are of great interest to investigate. Recent investigations have highlighted that the irradiation-induced defects of single-walled carbon nanotubes (SWCNTs) can be self-healed by annealing at an appropriate temperature, indicating that their healing is thermally activated.<sup>8</sup> Except for increasing the temperature, some chemical processes at the defective site, such as uploading external carbon sources,<sup>7,9</sup> are reported as a successful route to close the defect and return to original SWCNTs.

Point defects, for instance, atomic vacancies, are not favored thermodynamically because of their high formation energy. However, they can be easily introduced through electron or ion irradiation.<sup>10</sup> Such vacancies contain divalent, and thus highly reactive, carbon reaction centers. Accordingly, the addition of certain small molecules on the unsaturated carbon can be expected as particularly favorable. On the other hand, radiation-induced point defects are always recognized as one main reason that causes conductance loss,<sup>11</sup> or even changing the electric property from metallic to semiconducting,<sup>12</sup> because the radiation-induced defects act as an energy barrier for carriers.<sup>13</sup> Especially, when the vacancy is filled with a molecule through chemical bonding, it can induce a new impurity or a native atomic rearrangement that may significantly alter the pristine property of such materials.

More recently, inspired by the experimental facts<sup>14</sup> that CO disproportionation could be possibly utilized to cure defective

Received: November 8, 2011

Revised: December 28, 2011

Published: January 5, 2012



SWCNTs, Mercuri et al.<sup>9</sup> and Nongnual et al.<sup>7</sup> have proposed different CO-healing mechanisms that finally restore the SWCNTs, without creating any other new defect. Although the CO-healing process is thermoactivated and only in a theoretical point of view, since a heated flow of high-pressure CO is commonly used as a carbon source to grow carbon nanotubes (known as the HiPco method), it definitely provides new aspects to possibly cure the vacancy defect, rather than the current annealing method that is only based on the vacancy self-curing ability (a perfect tube cannot be reached anyhow). Comparing to the healing of defective SWCNTs, studies regarding the repair of graphene or graphene nanodots are scarce.

When detecting the electrical conductivity change of the sensor in practical applications, an electric field ( $F$ ) would be always present.<sup>5c</sup> It is well known that  $F$  can effectively modify the electronic structures and transport properties of low-dimensional systems, for instance, carbon nanotubes<sup>15</sup> and quantum wires.<sup>16</sup> However, to our knowledge, the corresponding atomic structure and adsorption property changes of graphene or a graphene nanodot under different strengths of  $F$  have not been investigated. Herein, by taking the applied  $F$  into account, we have explored the CO adsorption on the pristine graphene nanodot and the defective one systematically. Also, the feasibility of CO repairing the graphene nanodot with a monovacancy has been investigated. We do believe our results will shed light on the future development of graphene healing and gas sensing.

## ■ COMPUTATION METHODS

The defective structures and dynamics of carbon-based nanomaterials are discussed mostly from the theoretical point of view throughout the literature, due to a lack of suitable techniques to adequately access these areas.<sup>17</sup> Quantum mechanical methods have shown to be a feasible alternative to experiments in understanding the mechanisms of gas sensing and defect healing at the molecular level.<sup>18</sup> In this paper, we present first-principles calculations, through which we examine the  $F$  effects for CO adsorption on a pristine/defective graphene nanodot, and propose a viable strategy on vacancy healing. To computationally study all these, density functional theory (DFT) calculations were carried out using a suite of Gaussian 09 programs.<sup>19</sup> Among the tested hybrid meta exchange-correlation functionals, M06-2X provides the best results for the combination of main-group thermochemistry, kinetics, noncovalent interactions, and electronic excitation energies to valence and Rydberg states.<sup>20</sup> Hence, as a useful DFT method that shows the best performance in main-group thermochemistry and noncovalent interactions, M06-2X is sufficient to evaluate the CO adsorption and defect repair in our system. All the structure optimizations were performed using M06-2X with the 6-31G\* basis set. The integral=ultrafine option was utilized to minimize the integration grid errors that may arise from using an inadequate grid in the current M06 suite of functionals,<sup>21</sup> even though the default grid in Gaussian 09 is a fine grid, which is sufficient.

In this study, to minimize boundary effects on the energies of interest, a sheet of a square graphene nanodot was constructed as a basic substrate, which contains 116 carbon atoms in the perfect form and 115 carbon atoms in the defective form with a monovacancy positioned in the center. CO is initially placed near the central carbon hexagon. In addition, hydrogen atoms were used to terminate dangling carbon bonds at the substrate

edges for all cases. For the  $F$  condition, a finite dipole field with different strengths was applied perpendicular to the substrate plane. As to the adsorbed complex, both the positive and the negative field directions were considered. For the substrate itself, only one field direction was considered due to symmetry.

## ■ RESULTS AND DISCUSSION

To adequately investigate the sensing ability of the chosen graphene nanodot, it is essential to understand the interaction between the substrate surface and the adsorbate molecules. In this article, we mainly focus on the carbon monoxide adsorption on the selected substrate (if it is not specifically pointed out, it refers to the perfect form with no vacancy), although other small gas molecules,<sup>5d,22</sup> such as NO, NO<sub>2</sub>, NH<sub>3</sub>, and H<sub>2</sub>O, are also reported as possible adsorbates on a pristine graphene. We determine its preferential orientation on the substrate surface and its optimal adsorption site by calculating its adsorption energy. To find the most favorable adsorption configuration, a CO molecule is initially placed at different positions above the nanodot surface with a parallel or perpendicular orientation near the central carbon hexagon. The adsorption sites are generally divided into three categories, namely, the center of a carbon hexagon, the center of a carbon-carbon bond, and the top of a carbon atom. (The edge effects toward the adsorbate molecule also have been tested. Our results imply that the impacts of the two different edges are nearly identical with respect to the adsorption of a CO molecule near the same central carbon hexagon.) After full relaxation, the optimized configurations obtained from respective initial states are compared to identify the most energetically stable one. Figure 1 displays the optimized adsorption configurations after the removal of repeated geometries, and the corresponding adsorption energy ( $E_a$ ), equilibrium molecule-substrate distance ( $D$ , the shortest atom-atom distance), and Mulliken charge ( $Q$ ) of the CO adsorbed on the substrate are listed in Table 1.

As shown in Figure 1, the orientation of the CO molecule undergoes a slight change, indicating the parallel and perpendicular; these two highly symmetric orientations are favorable for CO adsorption to the graphene-like surface. As can be seen in Table 1, the calculated adsorption energies ( $E_a$ ) reflect that CO undergoes weak physisorption on the graphene nanodot, no matter whether the CO orientation is parallel or perpendicular to the substrate. However, the  $E_a$  values obtained through the parallel geometries are exclusively larger than the values obtained via the perpendicular ones. The energy difference in each category is small, which is in accordance with another report that the  $E_a$  is primarily determined by the orientation and to a lesser degree by the position of the molecule.<sup>5d</sup> The largest energy difference between each category is observed to be 0.061 eV, indicating that the parallel orientation for CO is indeed energetically more favorable than the perpendicular orientation. Moreover, the calculated equilibrium molecule-substrate distance also illustrates an orientation-dependent characteristic. Namely, the parallel category shows on average a smaller  $D$  value than that of the perpendicular one, leading to greater intermolecular interactions and thus larger  $E_a$ 's. It is worthy to notice that the shortest intermolecular distance is discerned in the perpendicular category, referring to the distance obtained from the close O-C contact (O atom from CO and the C atom from substrate), whereas most of the other  $D$ 's are obtained from the C-C contact. The smaller  $D$  value in the O-C contact does

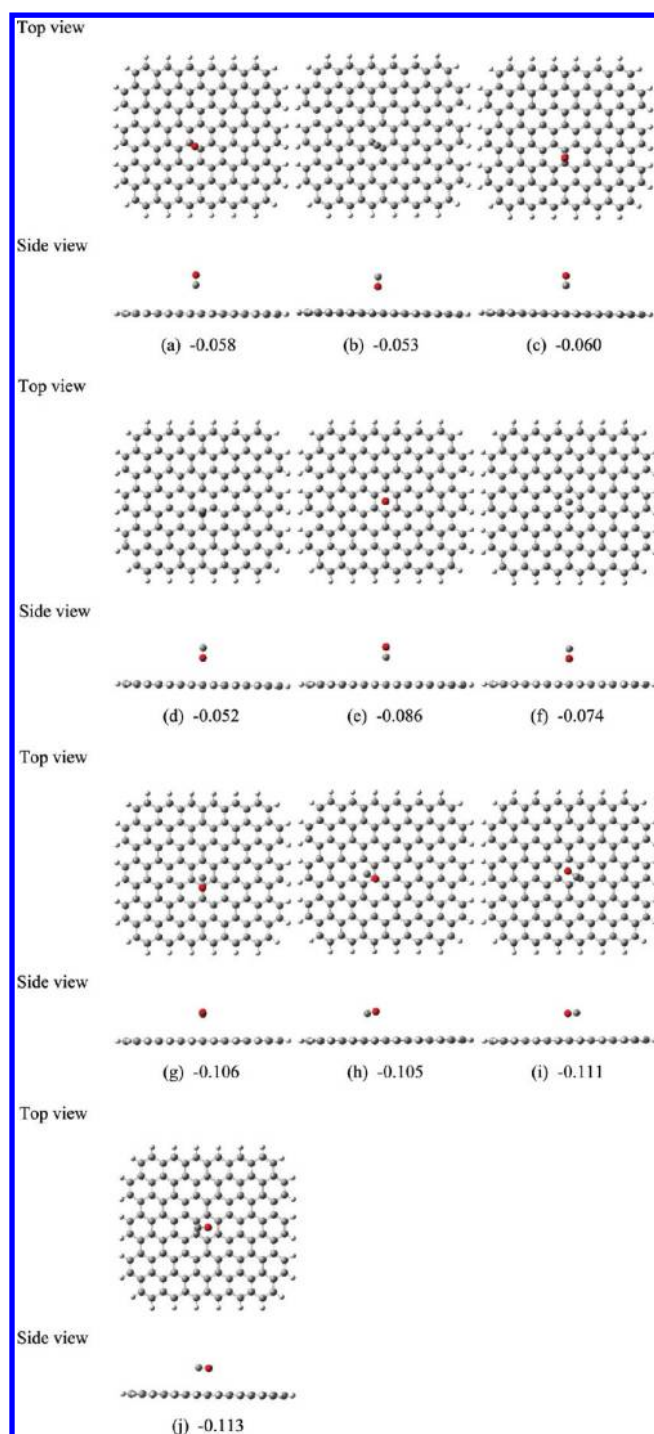


**Figure 1.** Ten configurations considered for a CO adsorbed graphene nanodot. Adsorption energies are given in electronvolts.

not increase the adsorption energy. The total electronic structure turns out to be less stable because a repulsive force becomes dominant when the electron-rich O atom approaches the graphene-like surface. The electron-rich graphene nanodot seems to function as an electron donor; in other words, the relatively electron-deficient C atom can accept the excessive charge and tunes the system to be more stable. This is further confirmed by Mulliken charge distribution analysis (Table 1). Among the tested configurations, j, with the adsorbed CO aligned along the axis of two opposite carbon–carbon bond centers in the six-membered ring, is found to be the most stable

**Table 1.** Adsorption Energy ( $E_a$ ), Equilibrium Molecule–Substrate Distance ( $D$ ), and Mulliken Charge ( $Q$ ) of the CO Adsorbed Graphene Nanodot

configuration		$E_a$ (eV)	$D$ (Å)	$Q^a$ (e)
CO⊥substrate	a	−0.058	3.374	−0.001
	b	−0.053	3.119 <sup>b</sup>	0.003
	c	−0.060	3.329	−0.001
	d	−0.052	3.059 <sup>b</sup>	0.002
	e	−0.086	3.402	−0.003
	f	−0.074	3.219 <sup>b</sup>	0.003
CO  substrate	g	−0.106	3.179	−0.005
	h	−0.105	3.199	−0.005
	i	−0.111	3.150	−0.004
	j	−0.113	3.189	−0.004

<sup>a</sup>A negative value means the electron transfer from the substrate to the adsorbed CO molecule. <sup>b</sup>Referring to the distance between the O atom from CO and the C atom from the substrate.

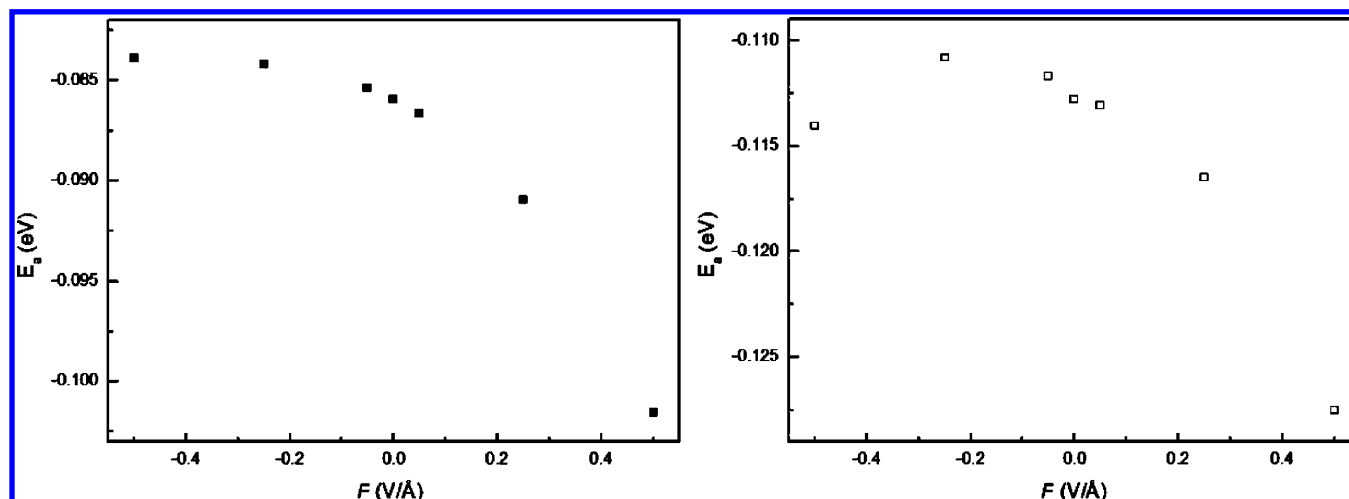
one ( $E_a = 0.113$  eV). This is different from the previous reference,<sup>23</sup> which demonstrates that the configuration i with the CO aligned toward the axis of two opposite C atoms in the six-membered ring is more stable. The charge transfer between the considered adsorbate and graphene nanodot is found to be almost independent of the adsorption site, but it does depend strongly on the orientation of the adsorbate with respect to the substrate surface. It is well known that CO is a relatively strong electron-donating molecule. However, most of our tested configurations elucidate that CO has a electron-withdrawing capacity rather than always acting as an electron donor.<sup>5d</sup> Only for the configurations b, d, and f, when O approaches the substrate, a very small charge is transferred from the CO to the substrate.

The electric field ( $F$ ) is known to effectively modify both the electronic structures and the transport properties of low-dimensional systems. However, these issues are not easily accessible by experimental methods. Consequently, quantum mechanical methods have shown to be a viable alternative to experiments in understanding the structure and property change under  $F$  at the molecular level. On the basis of the calculated  $E_a$  values, e and j, representing two different orientations, are chosen to explore the  $F$  effects. The positive direction of  $F$  is defined starting from the substrate toward the adsorbate. The corresponding  $E_a$ 's under different  $F$ 's are listed in Table 2. Our results reveal that, for both e and j, the positive  $F$  helps to enhance the  $E_a$ , and as  $F$  increases,  $E_a$  enhances evidently. The adsorption can be strengthened by the positive  $F$ , whereas the negative  $F$  only shows to have a small influence on  $E_a$  (Figure 2). The adsorption energy change can be explained by the shortest intermolecular distance  $D$  (referring to the C–C distance). As shown in Table 3,  $D$  decreases as we increase the strength of the positive  $F$ . However, the  $F$  along the negative direction displays a relatively less obvious impact on the  $D$  value. On the other hand, note that curvatures have been introduced to the graphene nanodot because of  $F$  (Figure 3). The degree of curvature is observed to be relevant with the strength of  $F$ . Considering our previous work on coronene, we have found that a steeper curvature can adsorb the molecule stronger on one side due to the more  $sp^3$  character of the carbon.<sup>24</sup> The  $E_a$  increases with the positive  $F$  can then be understood because the positive  $F$  provides a steeper curvature along the favorable adsorption site. To study the charge transfer between adsorbate and substrate under different  $F$ 's, we also carry out Mulliken



Table 2. CO Adsorption Energy  $E_a$  (eV) of Selected Configurations under Different  $F$ 

configuration	$F$ (V/Å)						
	−0.5	−0.25	−0.05	0	0.05	0.25	0.5
CO⊥substrate e	−0.084	−0.084	−0.085	−0.086	−0.087	−0.091	−0.102
CO  substrate j	−0.114	−0.111	−0.112	−0.113	−0.113	−0.116	−0.128

Figure 2. Variation of adsorption energy ( $E_a$ ) under the applied electric field for the configurations e (left) and j (right), respectively.Table 3. Equilibrium Molecule–Substrate Distance  $D$  (Å) under Different  $F$ 

configuration	$F$ (V/Å)						
	−0.5	−0.25	−0.05	0	0.05	0.25	0.5
CO⊥substrate e	3.416	3.413	3.403	3.402	3.400	3.383	3.351
CO  substrate j	3.197	3.141	3.169	3.189	3.183	3.140	3.111

charge analysis on the adsorbed CO molecule in configurations e and j, respectively (see Table 4). Our results demonstrate that, with increasing positive  $F$ , more electrons transfer from the substrate to the CO, which can be attributed to the increased electron-donating ability of the carbon ( $sp^2 \rightarrow sp^3$ ) near the adsorption area. In contrast, the negative  $F$  tends to drive the electrons from the CO to the substrate. Thus, an applied electric field can be utilized not only to influence the adsorption energy of the small molecule but also to control the charge transfer between the small molecule and the adsorbent.

Vacancy-type defects due to electron-beam damage are frequently observed in HR-TEM.<sup>6b,25</sup> It has been reported the monovacancy does indeed exist in carbon nanostructures for at least a few seconds. The vacancy is immobile and does not merge together during observation at room temperature.<sup>6b</sup> Nevertheless, theoretical investigations<sup>26</sup> also predict that the intraplanar relaxation is weak for a monovacancy. More recently on graphene, a vast majority of single vacancies, such as mono- and divacancies, have been successfully visualized by high-angle annular dark-field (HAADF) images acquired in a scanning transmission electron microscope (STEM);<sup>27</sup> mono- and divacancies are directly interpretable, whereas the well-known atomic rearrangement defect, the Stone–Wales defect, is not observed. To heal the vacancy, a carbon-containing molecule without H atoms is favorable because H atoms are supposed to be trapped at the vacancies easily and hard to remove. Inspired from the works done by Mercuri et al.<sup>9</sup> and Nongnual et al.,<sup>7</sup> we have explored the feasibility of the CO molecule acting as a

vacancy-healing agent. To computationally study this idea, we positioned a monovacancy in the center of the same graphene nanodot (the missing carbon atom is pointed out in Figure 4); the incoming CO molecule is initially placed above the monovacancy perpendicularly with the carbon atom pointing toward the vacancy center, since a lot of studies<sup>7,23,28</sup> have already elucidated that the vacancy–OC direction is unfavorable due to a repulsive force between the nucleophilic defect and the oxygen atom of the CO adsorbate. Our calculation also confirms that the system is subjected to a much higher approaching barrier in the vacancy–OC direction. The vacancy–CO direction is preferable for a nucleophilic attack to the carbon atom (partial positive charge) of the CO molecule. After calculation, we have found that the initial distance ( $d$ ) between the vacancy center and the carbon of CO is crucial for triggering the healing process. Our results show that, when  $d = 3$  Å, the CO molecule cannot reach the vacancy through relaxation, whereas when  $d = 1.5$  Å, the CO molecule remerges with the vacancy after relaxation without an energy barrier. This directly indicates that there exists an approaching barrier between the vacancy and the incoming CO molecule, which is estimated to be 18.8 kcal/mol through our calculation. This value is also comparable to the result (16.2 kcal/mol) reported by Xu et al.<sup>28</sup> Our result implies that, if the distance between the incoming CO and the defect site is not close enough, the CO molecule is still physisorbed to the defective substrate after relaxation unless an activation energy is given.

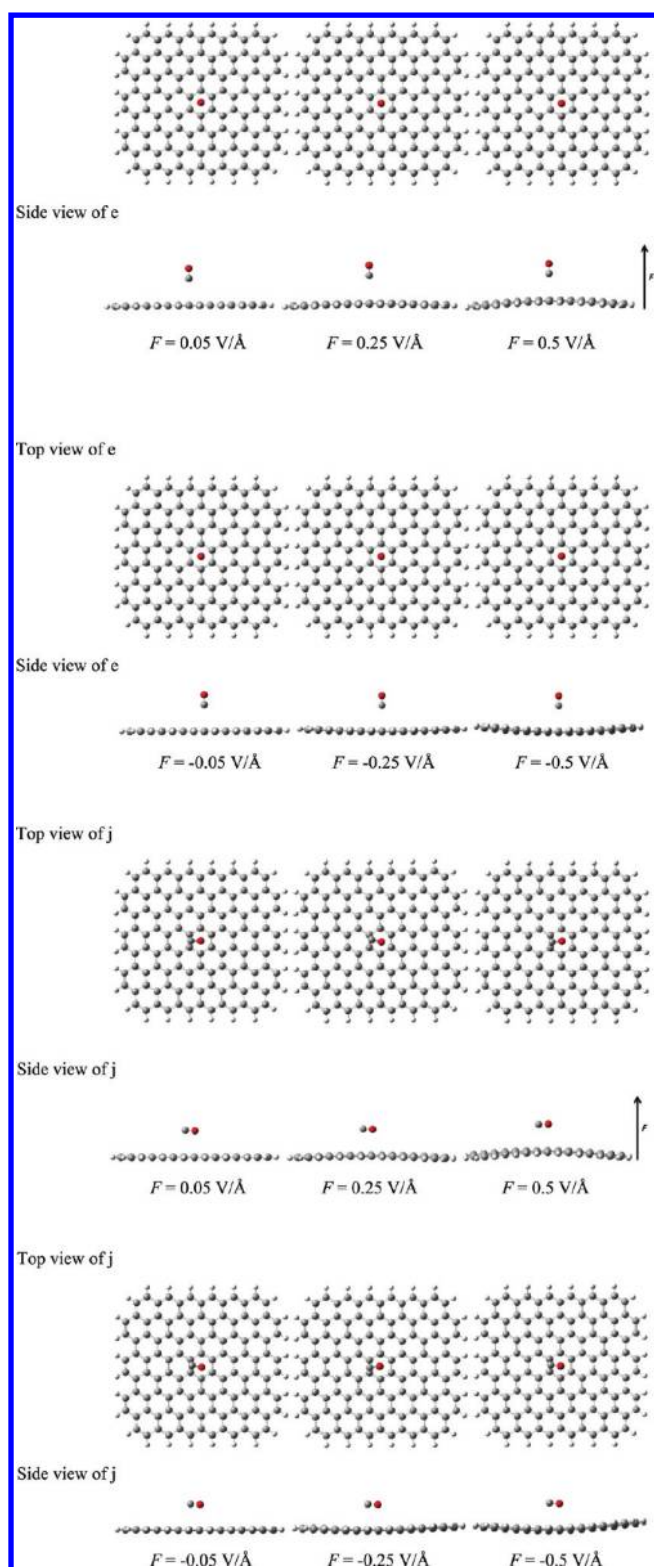


**Figure 3.** Structures of a CO adsorbed graphene nanodot under different electric fields ( $F$ ) (the positive direction of  $F$  is shown by the arrow).

To study the healing process of CO, we set the  $d$  value to be 1.5 Å (the closest distance between the carbon of CO and the carbon near the defect is measured to be 2.064 Å) and apply the electric field to the system to see how  $F$  affects the adsorption configuration. The optimized geometries are displayed in Figure 4 after full relaxation. We find that the CO molecule fills

**Table 4.** Mulliken Charge  $Q$  (e) of the CO Adsorbed on the Substrate under Different  $F$

configuration	$F$ (V/Å)						
	−0.5	−0.25	−0.05	0	0.05	0.25	0.5
CO⊥substrate e	0.004	0.001	−0.002	−0.003	−0.004	−0.008	−0.014
CO  substrate j	0.004	0.000	−0.003	−0.004	−0.005	−0.009	−0.016

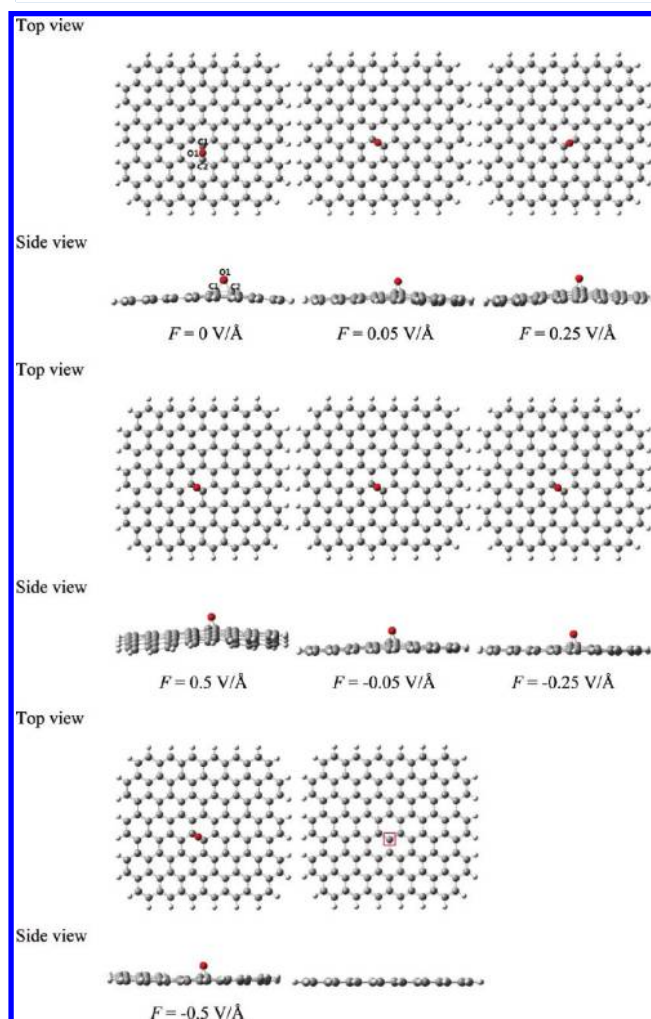


**Figure 4.** Structures of epoxide formed by adsorption of CO on the monovacant defect under different electric fields ( $F$ ). To clarify, the important atoms are labeled in the targeting structure for the later discussion on the removal of an O atom from the epoxy group. Also, the pristine graphene nanodot is shown for contrast, and the missing carbon atom is pointed out.

into the monovacancy and restores the hexagonal carbon network via the formation of a three-membered ring epoxide structure. Without an external electric field, the adsorption energy was calculated to be  $-5.84$  eV, which is comparable to a previously reported value of  $-6.3$  eV based on graphene,<sup>29</sup> indicating that a very strong chemisorption takes place. Considering that the CO adsorption energy on the pristine graphene nanodot was about 0.113 eV, it is believed, in equilibrium under the CO supply, that most of the monovacancies in graphene would be chemisorbed by CO and exist as epoxides. As can be noticed,  $F$  does affect the overall adsorption geometry; however, it can hardly block the formation of the epoxide structure. In view that the corresponding adsorption

energy variation is small under different  $F$ 's based on our calculation, it can be resulted from the remarkable stability that is provided by the bridging C–O–C bonds. The formation of the epoxy group has been predicted on the outer wall of CNTs in earlier theoretical work.<sup>9,30</sup> Additionally, for the defective graphene with a single vacancy, the creation of an epoxy group by exposure to CO was also confirmed by molecular dynamics simulations.<sup>28,29</sup> Note that, although the existence of an epoxy group repairs the carbon network of the monovacancy defective site, the newly created epoxide defect is believed to be very stable<sup>30,31</sup> and often causes conductivity loss.<sup>32</sup> It can be identified that, after the chemisorption of a CO molecule, the system becomes more semiconductor-like, with a 0.11 eV increase in energy gap. In addition, experiment has already confirmed the enhancement of graphene resistance upon CO exposure.<sup>33</sup> Because CO is proven to be weakly physisorbed to the pristine graphene surface and the charge transfer between them is small, the corresponding resistance change upon adsorption can be predicted to be minor. We believe the main reason for the increase of graphene resistance should be the chemisorption of CO to some chemical reactive sites, such as vacancies. To restore the original property of the pristine graphene nanodot, high temperature would be necessary to remove the oxygen atom by thermal annealing. Unfortunately, the required high-temperature annealing may result in holes in the basal plane of graphene.<sup>34</sup> On the basis of first-principles molecular dynamics simulations, Wang et al. have reported that NO can be a reactive molecule to remove the extra O from the epoxy group in graphene.<sup>29</sup> Here, we propose an alternative strategy to remove the unfavorable O atom through subsequent interaction with another CO molecule.

To explore the feasibility of the bimolecular healing strategy, we introduce a second CO molecule to the “half-healed” system

without an applied electric field for reducing complexity. The energy profile of the proposed reaction mechanism is illustrated in Figure 5, and the structural parameters corresponding to each reaction step are shown in Figure 6. The addition of CO to the epoxide (**1**) generated by CO chemisorption on the monovacant graphene nanodot leads to the formation of the reactant complex (**RC**), with an energy release of 3.37 kcal/mol. As can be seen, the bond lengths of C1–C2, C1–O1, and C2–O1 in **1** are 1.559, 1.415, and 1.416 Å, respectively. Upon adsorption (in **RC**), the bond lengths of C1–C2 and C2–O1 increase to 1.561 and 1.417 Å, respectively, whereas the bond length of C1–O1 is identical to that in **1**, indicating that the adsorption process weakens the epoxide structure and, compared with the C1–O1 bond, the C2–O1 bond is more likely to break if an activation energy is given. Note that the closest interatomic distance in **RC** is C3–O1, which is 2.857 Å, showing that the incoming CO molecule is still physisorbed on the “half-healed” system. The proposed reaction proceeds via the transition state (**TS**) with an activation energy of 33.4 kcal/mol. In comparison with the activation energy for this ring-opening process in the SWCNT (40.6 kcal/mol),<sup>9</sup> our result demonstrates that the removal of an O atom from the epoxide structure by the second CO molecule would be energetically much easier for the planar carbon network than the SWCNT. The C3 and O1 atoms are then bonded with a bond length of 1.688 Å. The bond length of the adsorbed CO is 1.156 Å, a little longer than that of the isolated molecule (1.131 Å), suggesting that the original C3–O2 bond is weakened due to the chemisorption. As predicted, the C2–O1 bond is broken with an atomic distance of 1.889 Å, while the bond length of C1–O1 increases to 1.505 Å. C1–C2 decreases to 1.486 Å, showing a tendency of the restoration to the pristine graphene hexagonal network. Once the epoxide structure is broken, the

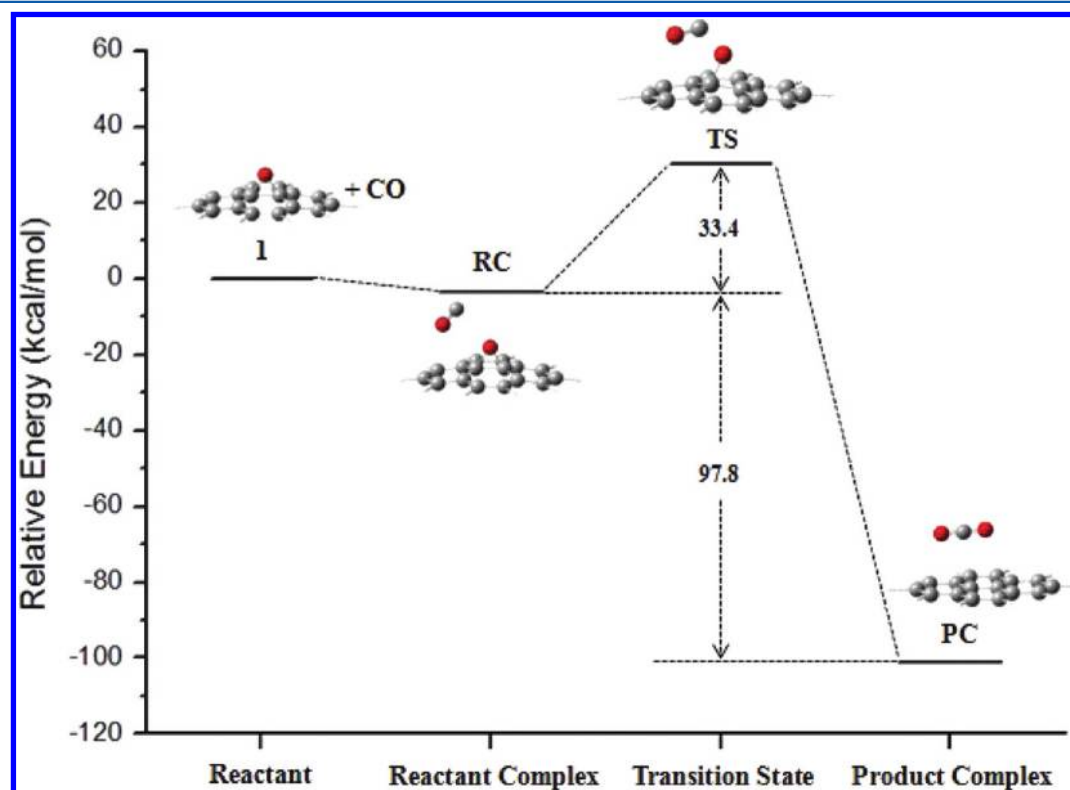


**Figure 5.** Energy profile of the vacancy-healing process. Reaction starts from the epoxide at the vacancy defect that interacts with an incoming CO molecule.



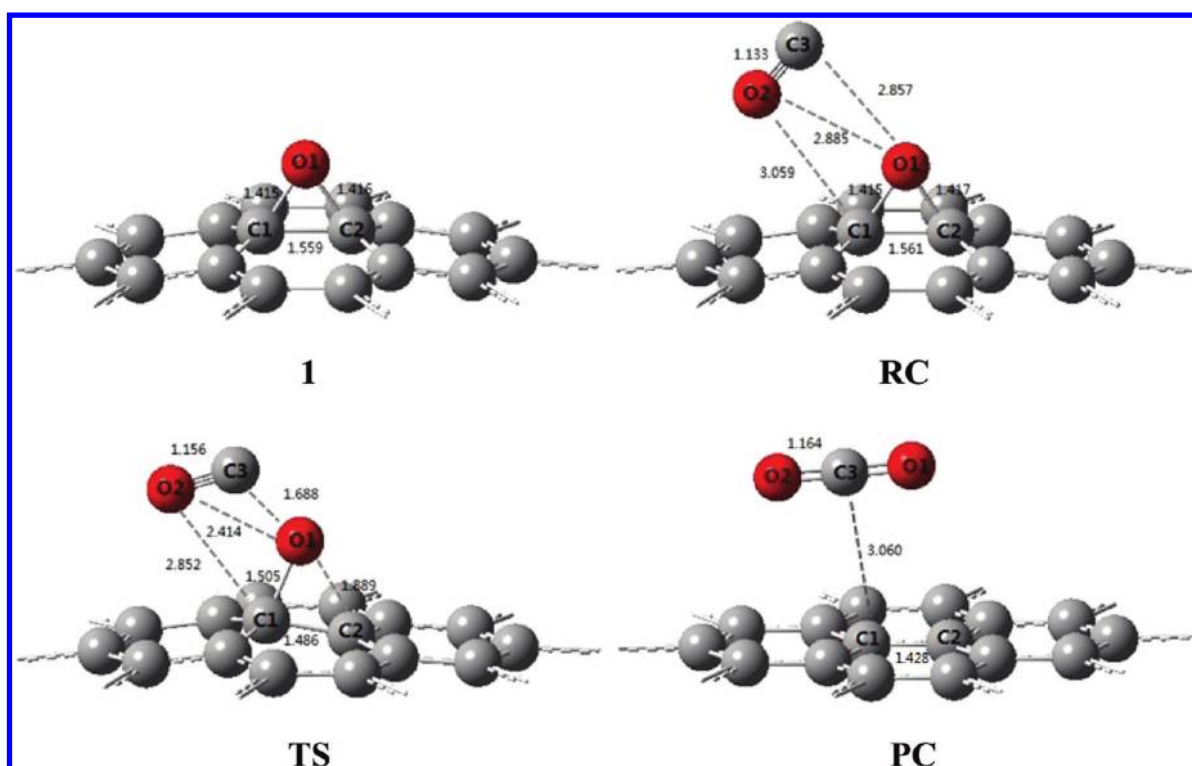


**Figure 6.** Optimized geometries of each step in the proposed reaction mechanism. The unit of selected bond lengths and interatomic distances is angstrom.

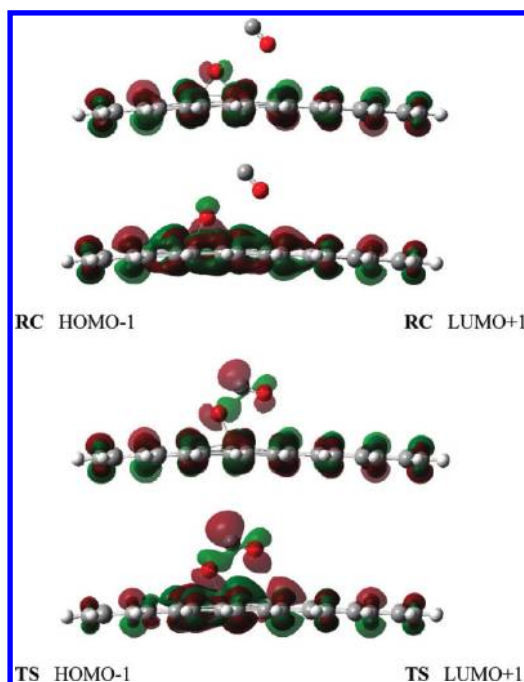


**Figure 7.** Selected frontier molecular orbital shapes of RC and TS.

dangling O atom is easily removed by the adsorbed CO through the formation of a CO<sub>2</sub> molecule. In the product complex (PC), the newly formed CO<sub>2</sub> lies parallel to the substrate with a closest carbon–carbon distance of 3.060 Å, which is consistent with the previous report 3.0 Å calculated on the basis of graphene.<sup>35</sup> The C1 and C2 atoms have also relaxed to the pristine hexagonal carbon network with a bond length of 1.428 Å, which is almost equivalent to that in graphene. Finally,

the addition of the CO molecule leads to the formation of a defect-free graphene nanodot and release of a molecule of CO<sub>2</sub> with an energy release of 131.2 kcal/mol.

To facilitate our understanding and give more insight into the reaction mechanism, we further looked into the frontier molecular orbitals of RC and TS from HOMO-3 to LUMO+3. Among the considered orbitals, HOMO-2 and LUMO+1 were found to be most responsible for the interactions between CO and the defective graphene nanodot (shown in Figure 7). The isolated CO molecule is bonded via the  $sp_z$ -hybridized orbital of a C atom and the  $p_z$  orbital of an O atom. Hence, an  $\sigma$ -bond is formed while the interaction between  $p_x$  and  $p_y$  orbitals of the C and O atoms induces two  $\pi$ -bonds.<sup>36</sup> However, a non-bonding electron lone pair in the C  $sp_z$ -hybridized orbital and a nonbonding electron lone pair in the O 2s orbital are left. Considering the adsorption configuration, when the C atom of CO approaches the O atom of the epoxy group, the nonbonding electron lone pair of C atom can first enter the antibonding molecular orbital of the O atom. After the C2–O1 bond breaks, the antibonding molecular orbital becomes a bonding orbital for the O–CO bond. Ultimately, a CO<sub>2</sub> molecule is formed.

## CONCLUSIONS

Here, we presented DFT calculations in understanding the adsorption of a CO molecule on a pristine graphene nanodot and the defective one with a monovacancy by taking the external electric field into account. It is found that the CO molecule is physisorbed to the pristine substrate, and there exists a recombination barrier (18.8 kcal/mol) for the incoming CO molecule remerging with the monovacancy. Our results also indicate that the CO adsorption process can be influenced by the applied  $F$ , and the positive  $F$  can be used to strengthen the CO adsorption. In addition, we proposed a reaction mechanism



for the subsequent healing of the monovacancy on the graphene nanodot by interaction with CO molecules. Our calculations provide a possible reaction pathway based on the formation of an epoxide intermediate upon the interaction of CO with the monovacancy. The subsequent interaction with the second CO molecule allows the restoration of the hexagonal network in the graphene nanodot with the release of CO<sub>2</sub>. Both processes are thermally activated, and the latter one is expected to overcome an energy barrier of 33.4 kcal/mol. In this work, the calculated results clarify the role of CO as an active chemical species to potentially cure the monovacancy defect. Although a lot of the other concerned issues, such as whether *F* can lower the activation barrier, or if other chemical species exist that are more energetically favorable for healing the monovacancy defect, are not engaged in this work, undoubtedly, we will continue to extend our effort to this interesting area and wish to give more insight in the future.

## AUTHOR INFORMATION

### Corresponding Author

\*Phone: +82-31-299-4560. Fax: +82-31-290-7075. E-mail: jinylee@skku.edu.

## ACKNOWLEDGMENTS

This work was supported by the National Research Foundation (NRF) Grants (2011-0001211 and 2011-0015767) funded by MEST. The authors would like to acknowledge support from the KISTI Supercomputing Center through the strategic support program for the supercomputing application research [No. KSC-2011-C2-52].

## REFERENCES

- (1) (a) Jang, S. R.; Vittal, R.; Kim, K. J. *Langmuir* **2004**, *2*, 9807. (b) Jitianu, A.; Cacciaguerra, T.; Benoit, R.; Delpeux, S.; Beguin, F. *Carbon* **2004**, *42*, 1147. (c) Miller, A. J.; Hatton, R. A.; Silva, S. R. P. *Appl. Phys. Lett.* **2006**, *89*, 123115. (d) Miller, A. J.; Hatton, R. A.; Chen, G. Y.; Silva, S. R. P. *Appl. Phys. Lett.* **2007**, *90*, 023105. (e) Kongkanand, A.; Dominguez, R. M.; Kamat, P. V. *Nano Lett.* **2007**, *7*, 676.
- (2) Ao, Z. M.; Zheng, W. T.; Jiang, Q. *Nanotechnology* **2008**, *19*, 275710.
- (3) (a) Novoselov, K. S.; Geim, A. K.; Morozov, S. V.; Jiang, D.; Zhang, Y.; Dubonos, S. V.; Grigorieva, I. V.; Firsov, A. A. *Science* **2004**, *306*, 666. (b) Berger, C.; Song, Z. M.; Li, X. B.; Wu, X. S.; Brown, N.; Naud, C.; Mayou, D.; Li, T. B.; Hass, J.; Marchenkov, A. N.; Conrad, E. H.; First, P. N.; de Heer, W. A. *Science* **2006**, *312*, 1191.
- (4) Stankovich, S.; Dikin, D. A.; Dommett, G. H. B.; Kohlhaas, K. M.; Zimney, E. J.; Stach, E. A.; Piner, R. D.; Nguyen, S. T.; Ruoff, R. S. *Nature* **2006**, *442*, 282.
- (5) (a) Kong, J.; Franklin, N. R.; Zhou, C. W.; Chapline, M. G.; Peng, S.; Cho, K. J.; Dai, H. J. *Science* **2000**, *287*, 622. (b) Collins, P. G.; Bradley, K.; Ishigami, M.; Zettl, A. *Science* **2000**, *287*, 1801. (c) Schedin, F.; Geim, A. K.; Morozov, S. V.; Hill, E. W.; Blake, P.; Katsnelson, M. I.; Novoselov, K. S. *Nat. Mater.* **2007**, *6*, 652. (d) Leenaerts, O.; Partoens, B.; Peeters, F. M. *Phys. Rev. B* **2008**, *77*, 125416.
- (6) (a) Banhart, F.; Kotakoski, J.; Krashenninnikov, A. V. *ACS Nano* **2011**, *5*, 26. (b) Hashimoto, A.; Suenaga, K.; Gloter, A.; Urita, K.; Iijima, S. *Nature* **2004**, *430*, 870.
- (7) Nongnual, T.; Limtrakul, J. *J. Phys. Chem. C* **2011**, *115*, 4649.
- (8) Karoui, S.; Amara, H.; Bichara, C.; Ducastelle, F. *ACS Nano* **2010**, *4*, 6114.
- (9) Mercuri, F. *J. Phys. Chem. C* **2010**, *114*, 21322.
- (10) (a) Kotakoski, J.; Krashenninnikov, A. V.; Kaiser, U.; Meyer, J. C. *Phys. Rev. Lett.* **2011**, *106*, 105505. (b) Krashenninnikov, A. V.; Nordlund, K. *J. Appl. Phys.* **2010**, *107*, 071301.
- (11) Suzuki, S.; Kobayashi, Y. *J. Phys. Chem. C* **2007**, *111*, 4524.
- (12) Vijayaraghavan, A.; Kanzaki, K.; Suzuki, S.; Kobayashi, Y.; Inokawa, H.; Ono, Y.; Kar, S.; Ajayan, P. M. *Nano Lett.* **2005**, *5*, 1575.
- (13) Kanzaki, K.; Suzuki, S.; Inokawa, H.; Ono, Y.; Vijayaraghavan, A.; Kobayashi, Y. *J. Appl. Phys.* **2007**, *101*, 034317.
- (14) Nasibulin, A. G.; Pikhitsa, P. V.; Jiang, H.; Kauppinen, E. I. *Carbon* **2005**, *43*, 2251.
- (15) (a) Li, Y.; Rotkin, S. V.; Ravaioli, U. *Nano Lett.* **2003**, *3*, 183. (b) O'Keeffe, J.; Wei, C. Y.; Cho, K. J. *Appl. Phys. Lett.* **2002**, *80*, 676.
- (16) Singh, J. *Physics of Semiconductors and Their Heterostructures*; McGraw-Hill Inc.: New York, 1993.
- (17) (a) Lee, G. D.; Wang, C. Z.; Yoon, E.; Hwang, N. M.; Kim, D. Y.; Ho, K. M. *Phys. Rev. Lett.* **2005**, *95*, 205501. (b) Ding, F.; Jiao, K.; Lin, Y.; Yakobson, B. I. *Nano Lett.* **2007**, *7*, 681. (c) Miyawaki, J.; Yuge, R.; Kawai, T.; Yudasaka, M.; Iijima, S. *J. Phys. Chem. C* **2007**, *111*, 1553. (d) Tsetseris, L.; Pantelides, S. T. *Carbon* **2009**, *47*, 901.
- (18) (a) Montoya, A.; Truong, T. N.; Sarofim, A. F. *J. Phys. Chem. A* **2000**, *104*, 8409. (b) Montoya, A.; Truong, T. T. T.; Mondragon, F.; Truong, T. N. *J. Phys. Chem. A* **2001**, *105*, 6757.
- (19) Frisch, M. J.; et al. *Gaussian 09*, revision B.01; Gaussian Inc.: Wallingford, CT, 2010.
- (20) (a) Zhao, Y.; Truhlar, D. G. *Theor. Chem. Acc.* **2008**, *120*, 215. (b) Zhao, Y.; Truhlar, D. G. *Acc. Chem. Res.* **2008**, *41*, 157.
- (21) Wheeler, S. E.; Houk, K. N. *J. Chem. Theory Comput.* **2010**, *6*, 395.
- (22) Wehling, T. O.; Novoselov, K. S.; Morozov, S. V.; Vdovin, E. E.; Katsnelson, M. I.; Geim, A. K.; Lichtenstein, A. I. *Nano Lett.* **2008**, *8*, 173.
- (23) Zhang, Y. H.; Chen, Y. B.; Zhou, K. G.; Liu, C. H.; Zeng, J.; Zhang, H. L.; Peng, Y. *Nanotechnology* **2009**, *20*, 185504.
- (24) Kang, B.; Kang, S.; Yan, S. H.; Lee, J. Y. *Bull. Korean Chem. Soc.* **2011**, *32*, 934.
- (25) Urita, K.; Suenaga, K.; Sugai, T.; Shinohara, H.; Iijima, S. *Phys. Rev. Lett.* **2005**, *94*, 155502.
- (26) (a) El-Barbary, A. A.; Telling, R. H.; Ewels, C. P.; Heggge, M. I.; Briddon, P. R. *Phys. Rev. B* **2003**, *68*, 144107. (b) Hjort, M.; Stafström, S. *Phys. Rev. B* **2000**, *61*, 14089.
- (27) Gass, M. H.; Bangert, U.; Bleloch, A. L.; Wang, P.; Nair, R. R.; Geim, A. K. *Nat. Nanotechnol.* **2008**, *3*, 676.
- (28) Xu, S. C.; Irle, S.; Musaev, D. G.; Lin, M. C. *J. Phys. Chem. C* **2009**, *113*, 18772.
- (29) Wang, B.; Pantelides, S. T. *Phys. Rev. B* **2011**, *83*, 245403.
- (30) Sorescu, D. C.; Jordan, K. D.; Avouris, P. *J. Phys. Chem. B* **2001**, *105*, 11227.
- (31) (a) Chen, Z. F.; Nagase, S.; Hirsch, A.; Haddon, R. C.; Thiel, W.; Schleyer, P. V. *Angew. Chem., Int. Ed.* **2004**, *43*, 1552. (b) Dag, S.; Gulseren, O.; Yildirim, T.; Ciraci, S. *Phys. Rev. B* **2003**, *67*, 165424.
- (32) Kamat, P. V. *J. Phys. Chem. Lett.* **2010**, *1*, 520.
- (33) Joshi, R. K.; Gomez, H.; Alvi, F.; Kumar, A. *J. Phys. Chem. C* **2010**, *114*, 6610.
- (34) Bagri, A.; Mattevi, C.; Acik, M.; Chabal, Y. J.; Chhowalla, M.; Shenoy, V. B. *Nat. Chem.* **2010**, *2*, 581.
- (35) Ghosh, A.; Subrahmanyam, K. S.; Krishna, K. S.; Datta, S.; Govindaraj, A.; Pati, S. K.; Rao, C. N. R. *J. Phys. Chem. C* **2008**, *112*, 15704.
- (36) Blyholder, G. *J. Phys. Chem.* **1964**, *68*, 2772.